

JOANNA ADAMCZYK<sup>1</sup>, DANUTA SMOLKA-DANIELOWSKA<sup>2</sup>,  
ARKADIUSZ KRZĄTAŁA<sup>3</sup>, TOMASZ KRZYKAWSKI<sup>4</sup>

## Rare earth elements, uranium, and thorium in ashes from biomass and hard coal combustion/co-combustion

### Introduction

Rare earth elements are very valuable in the modern economy because they are used in modern highly advanced technologies (Strzałkowska 2022). Of all REE, the most important are lanthanum (La), europium (Eu), erbium (Er) and neodymium (Nd) (Całusz-Moszek and Białecka 2013). The growing demand as well as the situation on the economic market result in the search for alternative sources of REE. The European Union has launched a new strategy to diversify access to rare earth materials used for electronics and consumer goods. Moreover, the new European Union's strategy assumes the obtaining of critical raw materials by recycling or reprocessing waste (European Commission 2020).

---

✉ Corresponding Author: Danuta Smolka-Danielowska; e-mail: danuta.smolka-danielowska@us.edu.pl

<sup>1</sup> University of Silesia, Katowice, Poland; e-mail: joanna.adamczyk@us.edu.pl

<sup>2</sup> University of Silesia, Katowice, Poland; ORCID iD: 0000-0002-7173-2546;  
e-mail: danuta.smolka-danielowska@us.edu.pl

<sup>3</sup> University of Silesia, Katowice, Poland; e-mail: arkadiusz.krzatała@us.edu.pl

<sup>4</sup> University of Silesia, Katowice, Poland; e-mail: toasz.krzykawski@us.edu.pl



© 2023. The Author(s). This is an open-access article distributed under the terms of the Creative Commons Attribution-ShareAlike International License (CC BY-SA 4.0, <http://creativecommons.org/licenses/by-sa/4.0/>), which permits use, distribution, and reproduction in any medium, provided that the Article is properly cited.

Fly ash is characterized by a very fine grain size and a well-developed development area, which increases the concentration of trace elements, including REY. Fly ash constitutes approx. 70–85% of the total mass of furnace waste (Smołka-Danielowska 2013) and the commercial power industry produces almost twenty million tons of it annually (GUS 2021). Research on the content of REE in fly ash has been conducted by various authors around the world (Franus et al. 2015; Zhou et al. 2016; Dai and Filkeman 2018; Smith et al. 2019; Huang et al. 2020; Rybak and Rybak 2021; Hower et al. 2021; Strzałkowska 2022). Fly ash from the combustion of hard coal and lignite seems to be a prospective source of secondary REE. It is estimated that the world's hard-coal fly ash contains an average of 404 mg/kg REE (Ketriss and Yudovich 2009). Strzałkowska (2022) determined the REE content in the range of 356–2721 mg/kg in hard-coal ashes in Poland, in the magnetic fraction of ashes from 187 mg/kg to 208 mg/kg, and in the ash fraction  $< 45 \mu\text{m}$ , the REE concentration range is 266–314 mg/kg. Franus et al. (2015) determined REE in ashes from the co-combustion of hard coal and biomass in the range of 379–394 mg/kg. The content of REE in fly ashes varies depending on the type of furnace and the efficiency of fume dedusting, the quantity and quality of used hard coal. Ashes from hard coal combustion in conventional furnaces contain REY in the range of 301.3–389.6 mg/kg, and in fluidized bed furnaces, in the range of 146.94–266.9 mg/kg (Smołka-Danielowska 2013; Adamczyk et al. 2018). The content of Y in fly ashes from hard-coal combustion ranges from 2.8 mg/kg to 233 mg/kg (Wdowin and Franus 2014; Adamczyk et al. 2018; Choudhary et al. 2022; Fu et al. 2022).

Jerzak et al. (Jerzak et al. 2021) found that the efficiency of retention of trace elements in ashes is influenced by the diameter of coal particles ( $< 600 \mu\text{m}$ ), and the size distributions of these particles are unimodal. The distribution and abundance of REE in hard coal vary regionally, e.g. in Chinese hard coal, the content of these elements is almost twice as high as the average world level (Ramakrishna et al. 2018).

Vassilev and Vassileva (Vassilev and Vassileva 2020) in ashes from sunflower husk and walnut shells determined the REE content at 5.95 mg/kg and 41.68 mg/kg (of which yttrium – 0.29 mg/kg), respectively. Sunflower husk pellets are often used in coal-fired power plants due to their high calorific value (21 MJ/kg), relatively low chlorine content and resistance to biodegradation (high lignin content – 34.17 wt.%) (Piyo 2014; Kałużynski et al. 2017; Zajemska et al. 2017). Walnut shells are a potential source of biomass as they make up almost 40% of the total weight of the fruit (Jahanban-Esfahlan et al. 2020). The world production of walnuts in the shell is, according to various authors, from 2 mln tons to 3.7 mln tons per year (Queirós et al. 2020; Miladinović et al. 2020). The waste weight of apple pomace ranges from 10% to 25% of the processed raw material. In Poland, apple pomace is largely processed into cattle feed or used in the production of alcohol (Masiarz et al. 2019).

Geochemically REE can be divided into three fractions, which include light – LREE (La, Ce, Pr, Nd, Sm), medium – MREE (Eu, Gd, Tb, Dy, and Y), and heavy – HREE (Ho, Er, Tm, Yb, and Lu) (Blissett et al. 2014). The classification is very useful for the description of REY in coal and its ashes. Seredin (Seredin 2010) developed the REY classification, which takes into account current market trends and a demand forecast for the coming years. This

classification is more useful for industry requirements. From REE, he distinguished critical elements (Nd, Eu, Tb, Dy, Y, Er), non-critical elements (La, Pr, Sm, Gd), and excessive elements (Ce, Ho, Tm, Yb and Lu). The ashes should contain as many critical REY as possible because they can then constitute the raw material most suitable for the recovery of critical raw materials. For this purpose, the prospective coefficient (Coutl) is also calculated as the ratio of the critical REY to the total amount of excessive REY in the hard-coal ash, according to the following equation (1) (Serdedin and Dai 2012).

$$\text{Coutl} = \frac{(\text{Nd} + \text{Eu} + \text{Tb} + \text{Dy} + \text{Er} + \text{Y}) / \sum \text{REY}}{(\text{Ce} + \text{Ho} + \text{Tm} + \text{Yb} + \text{Lu}) / \sum \text{REY}} \quad (1)$$

- ↵ Coutl – prospective coefficient,  
 $\sum \text{REY critical}$  – Nd, Eu, Tb, Dy, Y, Er,  
 $\sum \text{REY excessive}$  – Ce, Ho, Tm, Yb, Lu

The higher the ratio, the more the material can be considered as having potential for REE recovery.

The objective of the study is to determine the concentration and geochemical fractions of REE in ashes from the combustion/co-combustion of biomass from the agri-food industry and hard coal (share of biomass in the co-combustion process: 20%, 40% and 60%). Biomass, which constitutes a large group of waste in the production of apple products, walnuts and sunflower seeds, was selected for analysis. The objective was to determine the chemical composition of the ash particles to identify the source of REE, U and Th in the ashes. It can be hypothesized that ashes from the co-combustion of agri-food biomass and hard coal can be a potential raw material for REE recovery, regardless of the type and share of biomass in the combustion process. Recycling is a very important source of many critical materials, including REE from landfills and CHP ashes. It constitutes a promising method to reduce the harmful effects of the extraction of REE on the environment.

## 1. Research materials and methods

The research material consisted of three types of biomass and hard coal, which were fired at a temperature of 850°C. The biomass samples were dried at 80°C and then ground using the SM 300 cutting mill to a fraction of 250 µm. Hard-coal samples were ground in a porcelain mortar to a dusty fraction. Samples of biomass and hard coal were placed in a silite laboratory furnace, which is equipped with a fume discharge pipe. The total ash was obtained in the firing process, which was subjected to further analyses. Biomass samples came from the Polish agri-food industry (apple pomace, walnut shells and sunflower husks). The hard coal comes from the Upper Silesian Coal Basin (USCB) (Polish Mining Group).

In total, nine samples of biomass ash, two samples of hard coal ash and eighteen samples of ashes from the co-combustion of biomass (20%, 40%, and 60% share) and hard coal were analyzed. The designations of the test samples are presented in Table 1.

Table 1. Symbols of ash samples for analysis

Tabela 1. Symbole próbek popiołów do analiz

Sample symbol	Sample type	Sample symbol	Sample type
AP	Apple pomace ash	AP20 AP40 AP60	Ash from co-combustion of apple pomace (20%, 40%, and 60%) and hard coal
WS	Walnut-shell ash	WS20 WS40 WS60	Ash from co-combustion of walnut shell (20%, 40%, and 60%) and hard coal
SH	Sunflower-husk ash	SH20 SH40 SH60	Ash from co-combustion of sunflower husk (20%, 40%, and 60%) and hard coal
HC	Hard coal		

Analyses of REY, U, and Th concentrations were performed using the ICP-MS method in Vancouver, Canada (Bureau Veritas Mineral Laboratories) using the certified reference material: STD OREAS45E\_IG and STD OREAS501D.

The morphology and chemical composition of the ash particles containing REY, U, and Th were determined using a Quanta 250 and Phenom XL environmental scanning electron microscope, equipped with an EDS (Thermo Fisher Scientific) X-ray microanalyzer (Institute Natural Sciences, Sosnowiec, Poland). The preparations were prepared in the form of polished specimens.

The mineral composition of ashes from biomass and hard-coal combustion/co-combustion was determined by the X-ray diffraction method (XRD), using a PANalytical X-ray diffractometer, MPD X'PERT PRO PW3040/60 (Faculty of Natural Sciences, Sosnowiec, Poland). The estimated percentage content of ingredients in the ash was determined by the Rietveld method.

The analysis of the ash grain composition was performed using the Analysette 22 MicroTec analyzer, which operates with a measurement range of 0.01–2000  $\mu\text{m}$  (Faculty of Natural Sciences, Sosnowiec, Poland).

## 2. Results and discussion

### 2.1. REY, U, and Th content

The granulometric analysis of ashes from biomass firing showed that particles with a diameter of up to 100  $\mu\text{m}$  predominate, in the amount of about 81% (AP), 82% (WS) and 84% (SH). In the ashes from the co-firing of biomass (60%) with hard coal, the share of particles with a diameter of up to 100  $\mu\text{m}$  is the highest and amounts to 75–77%, and in the remaining samples, it is in the range of 70–72%.

Table 2 shows the values of REY concentrations in ashes from combustion/co-combustion of biomass and hard coal.

The share of critical REE in the samples of ashes from WS biomass (1.3 mg/kg) and SH biomass (1 mg/kg) is at a similar level, while a higher concentration of these elements was determined in the ash sample from AP biomass (38.7 mg/kg) (Table 2). Converted into the percentage of critical REE in the tested biomass ashes, their content is in the range of 29.4–32%. Higher concentrations of U (3.8 mg/kg) and Th (8.8 mg/kg) were determined in AP biomass ashes. In the remaining samples of WS and SH biomass ashes, U (0.1 mg/kg) and Th (0.2–0.3 mg/kg) values are low.

In the hard coal ash, the average REY content is 175 mg/kg, including the critical REY-45.3 mg/kg, which is 25.9%. The average concentration of U and Th is 6 mg/kg and 14 mg/kg, respectively. Żelazny et al. (2020) determined the average content of selected REE (Y, La, Ce, Pr, Nd, Sm, Gd, Tb, Dy, Er, Yb) in Polish hard coal in the range from 45.3 mg/kg to 56.1 mg/kg. In hard coal from the USCB, the uranium content ranges from 0.1 mg/kg to 8.5 mg/kg, and thorium from 0.1–14.9 mg/kg. According to Ketris and Yudovich (Ketris and Yudovich 2009), the content of U in the world's coals is 1.9 mg/kg and the content of Th is 3.3 mg/kg.

In the samples of AP60 and SH60 ashes, a significant decrease in the REY content (73.5 mg/kg and 91 mg/kg) was observed, compared to the ashes in which the biomass constituted 20% and 40%. Such a correlation was not found in the samples of WS60 ashes, because the average concentration of REY was determined at a similar level as in the WS20 ash sample (153.8 mg/kg and 145.2 mg/kg), and lower in the WS40 sample (109.4 mg/kg) (Table 2).

The calculated coefficient of variation in the range of 0–20% and 20–40% for rare earth elements and yttrium indicate a small and medium variation in the chemical composition of ashes from the combustion/co-combustion of biomass (Table 2).

Figure 1 shows the concentrations of LREE, HREE and MREE in ashes from biomass and hard coal combustion/co-combustion. All ashes from biomass combustion mainly contain LREE; however, a higher concentration was determined in apple pomace ash (AP – 96.5 mg/kg), and much lower was found in the remaining biomass ash (SH – 3 mg/kg and WS – 4.1 mg/kg). Hard-coal ash is enriched in LREE and MREE, as is ash from AP biomass

Table 2. Content of (mg/kg) REY, U, and Th in ashes from combustion/co-combustion of biomass and hard coal

Tabela 2. Zawartość (mg/kg) REY, U i Th w popiołach ze spalania/współspalania biomasy i węgla kamiennego

REY	Sample												
	AP	WS	SH	HC	AP20	AP40	AP60	WS20	WS40	WS60	SH20	SH40	SH60
Y	13.8	0.5	0.4	18.8	21.0	17.4	8.0	17.4	12.2	15.6	20.8	16.8	10.2
SD	5.25	0.02	0.02	4.77	5.32	4.66	6.21	4.55	4.05	4.21	6.38	4.12	4.33
VC	20	3	3	18	18	16	21	17	16	18	23	18	17
La	21.8	0.9	0.7	34.4	35.7	28.8	13.7	28.4	19.8	27.3	35.3	27.9	17.0
SD	8.23	0.02	0.05	10.12	9.18	7.55	6.28	8.82	7.12	9.16	12.15	10.62	8.12
CV	28	2	4	31	29	27	22	23	25	23	28	25	22
Ce	45.38	2.03	1.5	73.0	68.51	57.52	27.90	56.60	40.19	54.60	68.62	56.32	34.13
SD	18.12	0.12	0.14	16.12	21.31	17.12	11.34	16.23	15.28	14.32	19.77	12.88	17.03
CV	21	2	2	22	26	22	18	22	20	21	22	19	23
Pr	5.2	0.2	0.1	8.3	8.1	6.6	3.1	6.7	6.6	6.3	8.0	6.5	3.9
SD	1.88	0	0	2.12	1.67	1.93	1.66	1.73	1.88	1.73	1.69	1.55	1.42
CV	17	2	2	10	8	8	9	10	10	18	16	18	20
Nd	20.1	0.8	0.6	18.7	31.7	25.7	12.1	26.0	17.7	24.1	31.0	25.2	14.8
SD	8.82	0.08	0.06	7.81	10.12	10.56	9.43	11.52	8.29	10.77	11.23	9.16	7.56
CV	24	2	2	20	26	27	23	20	18	21	25	20	16
Sm	4.0	0.2	0.1	5.7	6.2	5.2	2.4	5.1	3.5	4.9	6.2	5.0	3.0
SD	1.12	0	0	1.05	1.11	1.32	0.19	1.33	0.23	1.23	1.61	1.25	0.54
CV	20	2	2	4	11	12	4	18	5	7	21	8	4
Eu	0.9	0.06	0.04	1.2	1.3	1.1	0.5	1.1	0.8	1.0	1.3	1.1	0.8
SD	0.33	0	0	0.29	0.32	0.88	0.14	0.83	0.25	0.89	1.31	0.99	1.18
CV	8	2	2	2	4	10	12	9	8	7	21	10	17
Gd	3.4	0.06	0.06	4.7	5.2	4.4	2.0	4.4	3.0	4.1	5.3	4.2	2.5
SD	2.06	0	0	2.37	2.44	2.12	1.89	2.05	2.27	2.33	2.65	2.11	1.84
CV	21	2	2	21	22	18	16	17	20	21	24	18	17
Tb	0.05	0.05	0.03	0.5	0.7	0.6	0.3	0.6	0.4	0.5	0.7	0.6	0.3
SD	0	0	0	0.05	0.05	0.05	0	0.04	0.02	0.05	0.06	0.04	0.02

REY	Sample												
	AP	WS	SH	HC	AP20	AP40	AP60	WS20	WS40	WS60	SH20	SH40	SH60
CV	2	2	2	4	4	12	4	8	10	14	18	12	11
Dy	2.6	0.03	0.03	4.0	4.0	3.3	1.6	3.4	2.3	3.0	3.9	3.2	2.0
SD	1.1	0	0	0.93	0.91	0.88	1.03	0.89	0.77	0.98	1.11	1.06	0.98
CV	16	1	1	15	17	21	18	18	21	17	23	18	16
Ho	0.5	0.03	0.03	0.8	0.7	0.6	0.3	0.6	0.4	0.6	0.7	0.6	0.4
SD	0.02	0	0	0.08	0.09	0.06	0.01	0.06	0.05	0.06	0.06	0.06	0.03
CV	4	0	0	4	4	2	4	7	4	4	6	6	6
Er	1.3	0.06	0.04	2.1	2.0	1.7	0.8	1.7	1.2	1.5	2.0	1.6	1.0
SD	0.71	0	0	0.88	0.81	0.84	0.56	0.85	0.72	0.82	0.96	0.78	0.55
CV	21	12	10	22	20	20	16	21	20	18	22	16	19
Tm	0.2	0.05	0.03	0.3	0.3	0.2	0.1	0.2	0.2	0.2	0.3	0.2	0.1
SD	0.15	0	0	0.17	0.27	0.14	0.11	0.25	0.11	0.13	0.22	0.14	0.16
CV	24	4	4	28	27	22	20	27	18	24	33	25	21
Yb	1.1	0.06	0.03	2.2	1.7	1.4	0.7	1.4	1.0	1.3	1.7	1.4	0.8
SD	0.55	0	0	0.62	0.49	0.46	0.44	0.58	0.36	0.44	0.51	0.41	0.33
CV	22	2	2	20	18	16	18	18	21	20	22	18	17
Lu	0.2	0.03	0.03	0.3	0.2	0.2	0.03	0.2	0.1	0.2	0.2	0.2	0.1
SD	0.08	0	0	0.09	0.09	0.08	0	0.08	0.06	0.09	0.19	0.16	0.09
CV	22	4	4	6	8	8	4	21	22	22	26	20	24
U	3.8	0.1	0.1	6.0	6.0	4.8	2.2	5.0	3.4	4.6	5.9	4.8	2.9
Th	8.8	0.3	0.2	14.0	14.8	11.8	5.7	12.1	8.3	11.1	14.7	11.6	7.1
REY	120.5	4.93	3.55	175.0	187.3	154.7	73.53	153.8	109.4	145.2	186.0	150.8	91.0
LREE	96.5	4.1	3.0	140.1	139.2	123.8	59.2	122.8	87.8	117.2	149.1	120.9	72.8
MREE	20.7	0.6	0.4	29.2	32.2	26.8	12.4	26.9	18.7	24.2	32.0	25.9	15.8
HREE	3.3	0.23	1.15	5.7	15.9	4.1	1.93	4.1	2.9	3.8	4.9	4.9	2.4
Coutf	0.82	0.656	0.679	0.59	0.85	0.84	0.802	0.802	0.83	0.80	0.83	0.832	0.82
LaN/YbN	1.4	1.0	2.0	1.1	1.6	1.5	1.0	1.5	1.5	1.5	1.5	1.5	1.6
GdN/YbN	1.8	3.0	2.0	1.2	1.8	1.8	1.2	1.8	1.8	1.8	1.8	1.7	1.8
LaN/GdN	0.8	1.0	1.0	0.9	0.9	0.7	0.9	0.9	0.8	0.8	0.8	0.8	0.9

SD – standard deviation; CV – coefficient of variation.

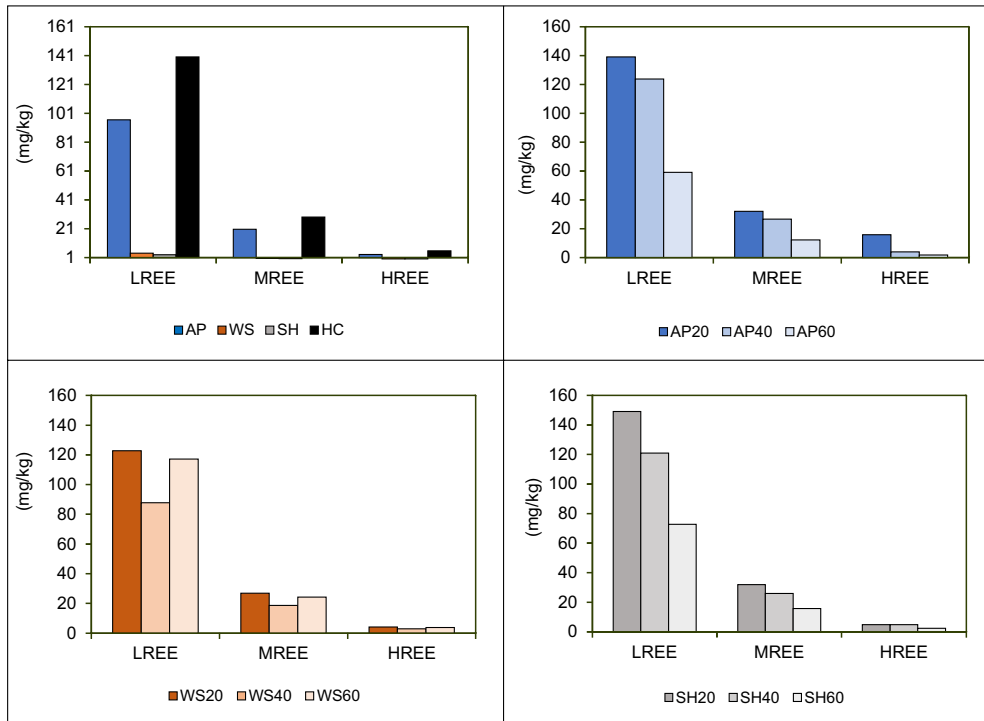


Fig. 1. Content of (mg/kg) LREE, MREE, and HREE in samples of ashes from combustion/co-combustion of biomass and hard coal

Rys. 1. Zawartość (mg/kg) LREE, MREE i HREE w próbkach popiołów ze spalania/współspalania biomasy i węgla kamiennego

(Figure 1). The HREE content in the tested samples is low, amounting to 5.7 mg/kg in the HC ash sample and 3.3 mg/kg in the AP ash sample.

The samples of WS (50.5%) ashes were found to have higher excessive values compared to the remaining ashes from the biomass AP and SH (Figure 2). In the samples of WS20 and WS60 ashes, the average content of critical REE was 49.8 mg/kg and 45.5 mg/kg, respectively, and non-critical was 44.6 mg/kg and 42.6 mg/kg, respectively, which is at a similar level (Figure 2). A lower content of these elements was determined in the WS40 ash sample (critical 34.2 mg/kg and non-critical 32.9 mg/kg) (Figure 2). Higher excessive REE values were found in the samples of WS20, WS40 and WS60 ashes compared to the remaining ashes from the co-combustion of HC with AP and HC with SH. The share of critical REE (Nd, Eu, Tb, Dy, Y, and Er) in the hard-coal ash samples is 25.9%. In the samples of ashes from biomass and hard coal co-combustion, the content of critical REE is on the average level of approx. 31%. In the samples of ashes from biomass, the content of critical REE is on the average level of approx. 28.8%. According to Rybak and Rybak (Rybak and Rybak



2021), fly ash from hard-coal combustion contains a higher fraction of critical REE (> 30%) in comparison to the total concentration of REE.

Hard coals are characterized by a high variability in the concentration of rare earth elements, because REE is bound to both the organic and mineral matter of coal. The REY content determined in the tested hard coal is 175.0 mg/kg. Enrichment of ashes from the co-combustion of biomass with REY may result from the presence of glass aluminosilicate and the organic substances in them (Fu et al. 2022). Its content in ashes can vary from 0.01 to 35.6% (Mattigod 2003; Eskenazy and Stefanova 2007; Anshits et al. 2010). An important role may be played by gas reactions on the surface of ash particles. The current state of research does not allow for an unequivocal solution to this problem.

The concentration of U and Th in the samples of ashes from the co-combustion of HC and AP as well as HC and SH decreases with the greater share of biomass in the combustion process, except for WS20 and WS60 ashes (Table 2).

The calculated values of the prospective factor for REY for the ash from firing walnut shells (Coutl = 0.66) and sunflower husks (Coutl = 0.69) are similar. A higher Coutl coefficient (0.82) was calculated in apple pomace ash (Table 2). In the samples of ashes from the co-combustion of hard coal and biomass, the calculated values of Coutl do not vary much

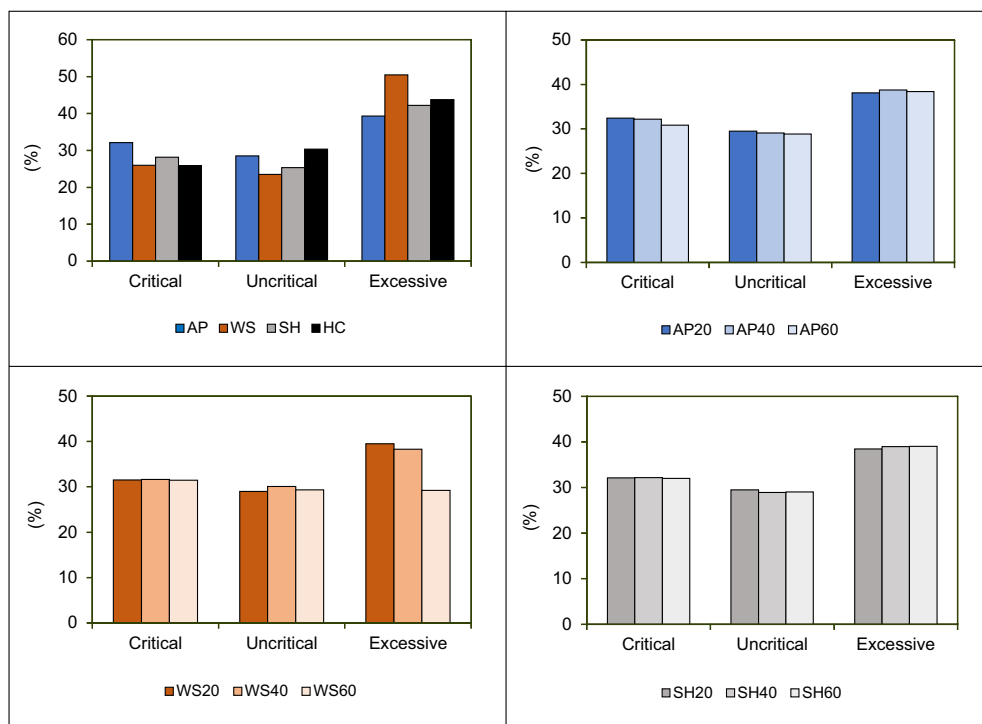


Fig. 2. Content of (mg/kg) REY in the tested ash samples due to the perspective criterion

Rys. 2. Zawartość (mg/kg) REY w badanych próbkach popiołów ze względu na kryterium perspektywiczne

and are within the range of 0.80–0.85 (Table 2). Ashes from AP biomass and ashes from the co-combustion of biomass and hard coal should be considered as potentially promising REY raw materials.

Table 3 presents Pearson's coefficients ( $r = 0.00$ – $0.10$  insignificant correlation;  $r = 0.10$ – $0.39$  weak correlation;  $r = 0.40$ – $0.69$  moderate correlation;  $r = 0.70$ – $0.89$  strong correlation;  $r = 0.90$ – $1.00$  very strong correlation) (Schober et al. 2018) determining the linear correlation between  $\sum U + Th$  and the content of LREE, HREE. In addition, Table 3 contains the calculated Pearson coefficients between the Y content and the concentration of MREE and critical REE.

Table 3. Pearson's correlation coefficients determine the linear correlations between the concentration of  $\sum U + Th$  and REE ( $n = 6$ ), and between the content of Y and REE ( $n = 8$ )

Tabela 3. Współczynniki korelacji Pearsona określające liniowe zależności pomiędzy koncentracją  $\sum U + Th$  a REE ( $n = 6$ ) oraz pomiędzy zawartością Y i REE ( $n = 8$ )

Sample	$\sum U + Th$			Y			
	LREE	HREE	Critical REE	LREE	MREE	HREE	Critical REE
AP	0.68	0.85	0.91	0.94	0.89	0.79	0.93
WS	0.96	0.975	0.95	0.69	0.62	0.97	0.78
SH	0.93	0.33	0.74	0.79	0.51	0.88	0.95
AP20	0.97	0.98	0.94	0.94	0.99	0.74	0.98
AP40	0.96	0.95	0.91	0.86	0.87	0.73	0.98
AP60	0.41	0.83	0.95	0.97	0.85	0.77	0.96
WS20	0.94	0.94	0.97	0.96	0.73	0.69	0.93
WS40	0.98	0.85	0.94	0.91	0.94	0.77	0.87
WS60	0.76	0.51	0.37	0.83	0.85	0.80	0.79
SH20	0.69	0.87	0.95	0.94	0.98	0.57	0.93
SH40	0.54	0.74	0.98	0.87	0.98	0.79	0.94
SH60	0.35	0.96	0.97	0.89	0.95	0.62	0.93

The tested ash samples from WS biomass combustion are characterized by a very strong and strong linear correlation between  $\sum U + Th$  and the content of LREE, HREE, and critical REE. In the case of ash from AP biomass, a moderate correlation was found between  $\sum U + Th$  and LREE content. A sample of SH biomass ash is characterized by a poor linear correlation between  $\sum U + Th$  and the HREE content (Table 3). In all samples of biomass ashes, a strong and very strong correlation was found between Y and the content of HREE and critical REE.

A weak correlation between  $\sum U + Th$  and the content of critical REE was found in the ashes of the WS60 sample ( $r = 0.37$ ), while between  $\sum U + Th$  and the content of HREE, the Pearson's coefficient is  $r = 0.51$  (Table 3). In the remaining samples of ashes from biomass and hard-coal co-firing, the linear correlation between  $\sum U + Th$  and the HREE content is strong and very strong. The strong correlation between Y and MREE concentration suggests that it is primarily the dysprosium and gadolinium content that influences the value of the “r” coefficient.

The concentration of REE in the samples of ashes from biomass and hard-coal combustion/co-combustion was normalized to the content of REE in the upper continental crust (UCC) in order to show the distribution pattern of individual REE in the tested ashes (Figure 3 and 4). Normalization and comparative parameters facilitate the graphical comparison of REE patterns between different types of ashes. To evaluate the suitability of the tested ashes as a potential REY raw material, three distribution schemes were adopted: LREY-L type (light type  $La_N/Lu_N > 1$ ), enriched with MREY-M type (medium type  $La_N/Sm_N < 1$  and  $Gd_N/Lu_N > 1$ ), and enriched with HREY-H type (heavy type  $La_N/Lu_N < 1$ ) (Seredin and Dai 2012). The calculated ratios of  $La_N/Yb_N$ ,  $La_N/Gd_N$  and  $Gd_N/Yb_N$  are represented as functions of LREE to HREE, LREE to MREE and MREE to HREE, respectively. Ce and Eu anomalies were defined as  $Ce/Ce^* = Ce_N/(La_N \times Pr_N)^{0.5}$  and  $Eu/Eu^* = Eu_N/(Sm_N \times Gd_N)^{0.5}$ .

Significant depletion or enrichment in LREE compared to HREE ( $La_N/Yb_N = 1.0$ – $2.0$ ) was found in all samples of ashes from biomass firing. Samples of these ashes are also characterized by a moderate MREE enrichment ( $Gd_N/Yb_N = 1.8$ – $3.0$ ;  $La_N/Gd_N = 0.8$ – $0.1.0$ ). Samples of biomass ash from WS and SH should be classified as type H, and biomass ash

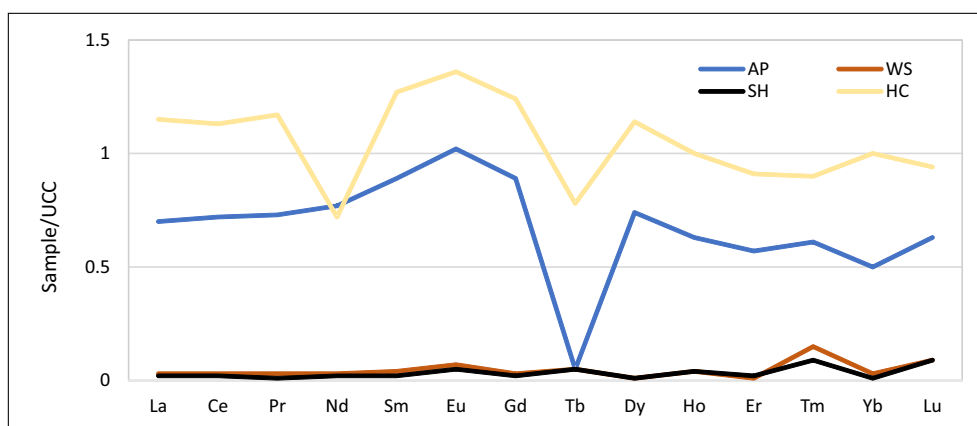


Fig. 3. Normalized concentrations of REE against UCC (upper continental crust) for samples of ashes from biomass and hard-coal combustion (UCC data is from Taylor and McLennan 1985)

Rys. 3. Znormalizowane stężenia REE względem UCC (górną skorupę kontynentalną) dla próbek popiołów ze spalania biomasy i węgla kamiennego (UCC znormalizowane wg Taylor i McLennan 1985)

samples from AP should be classified as mixed type L-M. In the biomass ash sample from AP, a positive Eu anomaly ( $\text{Eu}/\text{Eu}^* = 1.02$ ) and a clearly negative Tb anomaly were found (Figure 3). Positive anomalies of Pr, Sm, Gd, Dy, and Yb were found in hard-coal ashes.

On the basis of the curves of normalized REE concentrations in ashes from biomass and hard-coal co-firing, three groups of ashes can be conventionally distinguished (Figure 4):

- ◆ Group 1: AP20 and SH20;
- ◆ Group 2: AP40, SH40, WS20 and WS60;
- ◆ Group 3: AP60, WS40, and SH60.

All samples of ashes from biomass and hard-coal co-combustion are classified as type L-M, with the exception of WS20 ash samples (type L). The curves of normalized REE concentrations in the ashes of the first group (AP20 and SH20) are very similar to each other. Clearly positive Ce, Pr, Nd, Sm, Gd, Tb and Dy, Eu and Dy anomalies were found (Figure 4). In the second group of ashes, positive Sm and Gd anomalies and Nd were found in the WS20 ash sample (Figure 4). In the third group of ashes, positive anomalies were found for Pr (WS40) and Eu (SH60), and a strong negative one for Lu (AP60).

Ash from the combustion of biomass of agricultural and food origin (AP and SH) has good parameters regarding REY concentrations and the calculated prospective Coult coefficient. However, the optimal share of these types of co-fired biomass should be a maximum of 40%. The strong relationship between HREE and Y in WS and SH biomass ashes suggests that heavy rare earths are also bound by a small amount of unburnt organic matter. It is also found that the relationship between the concentration of HREE and Y may affect the content of terbium, which is more strongly associated with coal organic matter (Eskenazy and Stefanova 2007). The strong relationship between LREE and U and Th in ashes from biomass

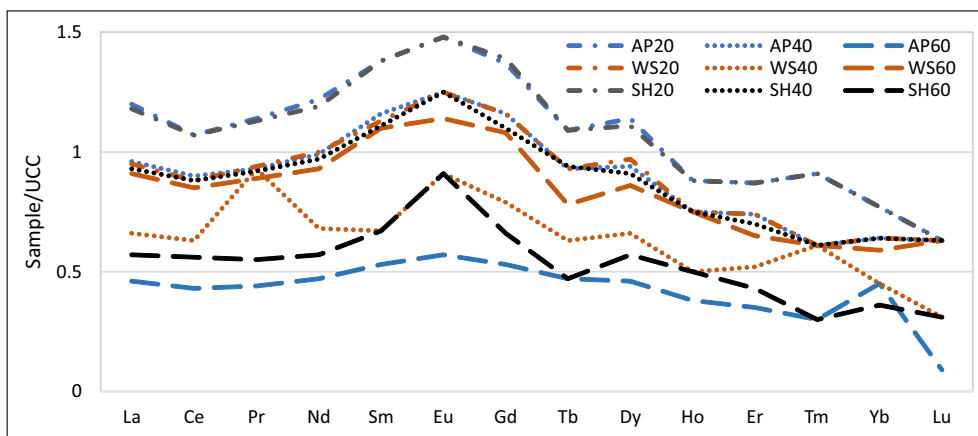


Fig. 4. Normalized concentrations of REE in relation to UCC (upper continental crust) for ashes from biomass and hard-coal co-combustion (UCC data are from Taylor and McLennan 1985)

Rys. 4. Znormalizowane stężenia REE względem UCC (górną skorupę kontynentalną) dla popiołów ze współspalania biomasy i węgla kamiennego (UCC znormalizowane względem Taylor i McLennan 1985)

co-firing (20% and 40% share) can be explained by the higher concentration of thorium, which is a component of monazite [ $\text{Ce}(\text{CePO}_4)$ ].

The results of REY concentrations presented in the study constitute the basis for further research, especially research based on fly ashes from fluidized bed furnaces. The appropriate selection of biomass from the agricultural and food industry and its share in the co-combustion process can significantly affect the REY content in ashes and the potential for their recycling.

## 2.2. Results of XRD and SEM-EDS analysis

The main minerals in ashes from the combustion of sunflower husks (SH) are arcanite (58.2%) and periclases (18.1%), the rest are pyroxenes, dolomite and calcite, and the amorphous substance. Quartz was determined in apple pomace ashes (AP), and dolomite and calcite were found in walnut shell ashes (WS). In all samples of ashes from biomass combustion, the amorphous vitreous phase was determined.

In the mineral composition of ashes from the co-combustion of biomass and hard coal, the main components determined are quartz, hematite, anhydrite, and calcite (Table 4). The vitreous and porous aluminosilicate phase occurs in a variable amount, depending on the type of biomass.

Auxiliary components in the tested ashes included periclase (MgO), dolomite [ $\text{CaMg}(\text{CO}_3)_2$ ], ilmenite ( $\text{FeTiO}_3$ ), magnetite ( $\text{Fe}_3\text{O}_4$ ), diopside ( $\text{CaMgSi}_2\text{O}_6$ ), akermanite [ $\text{Ca}_2\text{Mg}(\text{Si}_2\text{O}_7)$ ], gehlenite [ $\text{Ca}_2\text{Al}(\text{AlSiO}_7)$ ], magnesioferrite ( $\text{MgFe}_2\text{O}_4$ ), muscovite [ $\text{KAl}_2(\text{AlSi}_3\text{O}_{10})(\text{OH})_2$ ], and quandilite [ $(\text{MgFe})_2(\text{TiFe,Al})\text{O}_4$ ].

Table 4. Main minerals (%) in ash from biomass and hard-coal co-combustion

Tabela 4. Minerale główne (%) w popiołach ze współpalania biomasy i węgla kamiennego

Mineral component	Sample symbol								
	AP20	AP40	AP60	WS20	WS40	WS60	SH20	SH40	SH60
Quartz ( $\text{SiO}_2$ )	25.2	27.6	30.4	21.9	31.8	30.4	31.2	29.9	42.0
Hematite ( $\text{Fe}_2\text{O}_3$ )	–	–	–	43.1	19.2	12.8	17.4	29.6	13.5
Protohematite [ $\text{Fe}_{2-x}(\text{OH})_x\text{O}_{3-x}$ ]	23.3	25.1	18.6	–	–	–	–	–	–
Anhydrite ( $\text{CaSO}_4$ )	22.3	21.5	23.6	24.0	27.1	25.8	26.0	24.4	22.9
Calcite ( $\text{CaCO}_3$ )	10.3	8.6	11.8	11.0	8.6	12.2	12.9	8.7	11.9

The SEM-EDS studies show that ashes from biomass firing contain yttrium ( $Y_2O_3$ ) (Figure 5 A–B) and thorium ( $ThO_2$ ) (Figure 5C). Yttrium coexists with calcium oxides of

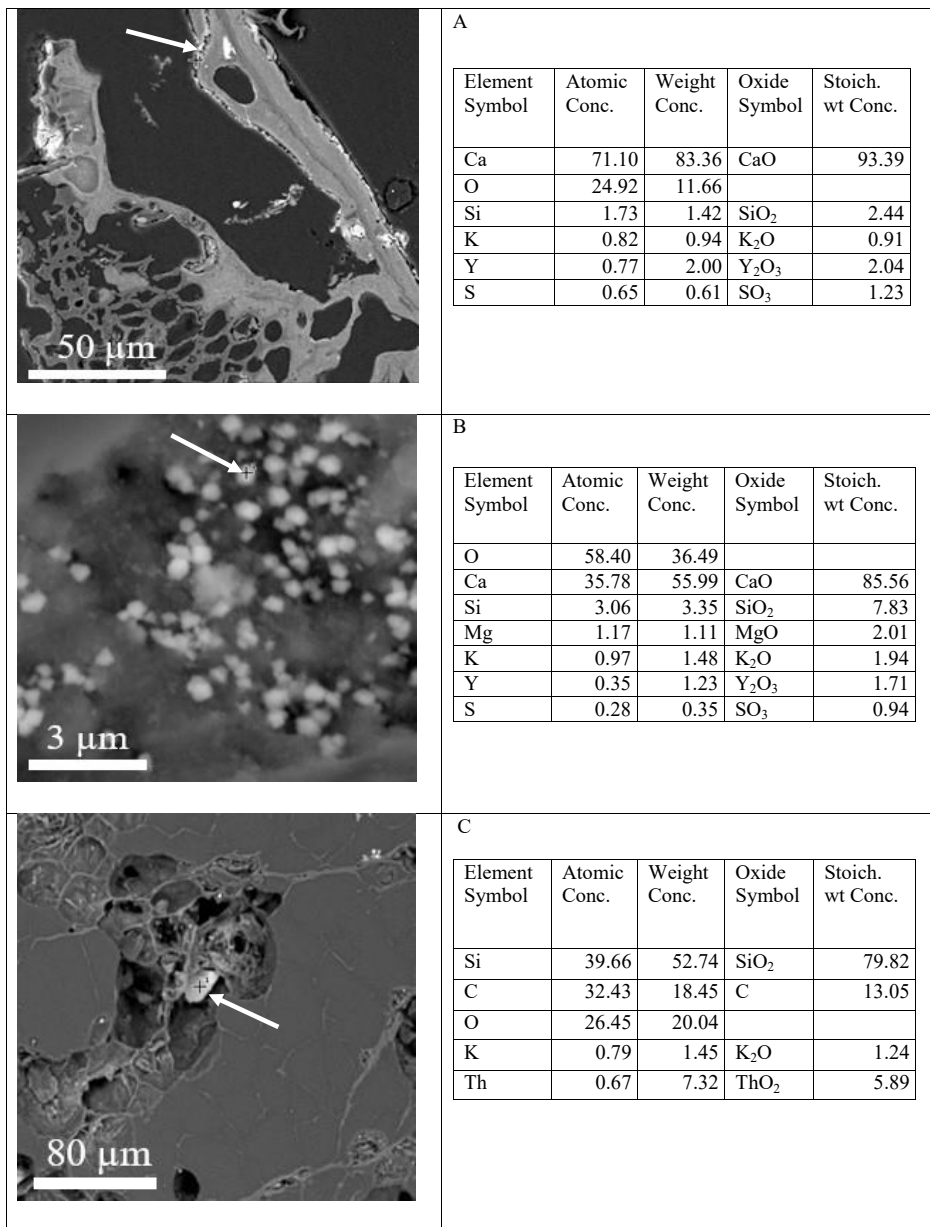


Fig. 5. Sample images from the scanning electron microscope (SEM) and the chemical composition of ash particles from biomass combustion (A, C – apple pomace; B – sunflower husk)

Rys. 5. Przykłady zdjęć ze skaningowego mikroskopu elektronowego (SEM) i skład chemiczny cząstek popiołów ze spalania biomasy (A, C – wytloki z jabłek; B – łuski słonecznika)

various morphological forms. Calcium oxides contain admixtures of Si, K, Mg, and S, and their amount is variable and small (Figure 5A, B). Calcium oxides often fill the pores in the unfired remnant of the tissue that makes up the biomass. In the chemical composition of ashes from biomass combustion, the content of  $Y_2O_3$  is in the range of 1.71–5%. The yttrium-containing ash particles are small, most of them are about 1  $\mu\text{m}$  and less. Thorium ( $ThO_2$  below 6%), which occurs in association with quartz in the pores of unfired tissue, was also determined in the particles of ash from biomass combustion. Thorium was determined only in the AP ash samples (Figure 5C).

Yttrium coexists with calcium oxides of various morphological forms. Calcium oxides contain admixtures of Si, K, Mg and S, and their amount is variable and small (Figure 5A, B). Calcium oxides often fill the pores in the unfired remnant of the tissue that makes up the biomass. In the chemical composition of ashes from biomass combustion, the content of  $Y_2O_3$  is in the range of 1.71–5%. The yttrium-containing ash particles are small, most of them are around 1  $\mu\text{m}$  and less. Thorium ( $ThO_2$  below 6%), which occurs in association with quartz in the pores of unfired tissue, was also determined in the particles of ashes from biomass combustion. Thorium was determined only in the AP ash samples (Figure 5C).

In the particles of ashes from the co-combustion of biomass and hard coal, xenotime-Y ( $YPO_4$ ) and zircon ( $ZrSiO_4$ ) (Figure 6A), and monazite-Ce ( $CePO_4$ ) (Figure 6B) were observed.

Xenotime and zircon grains were mainly observed in samples of WS20, WS40, and WS60 ashes. Xenotime is present in the form of single grains and in aggregates with sizes ranging from a few to several dozen  $\mu\text{m}$ . Monazite grains are sharp-edged, cracked and often show traces of dissolving. Monazite sizes range from 5  $\mu\text{m}$  to 20  $\mu\text{m}$ . Most of them

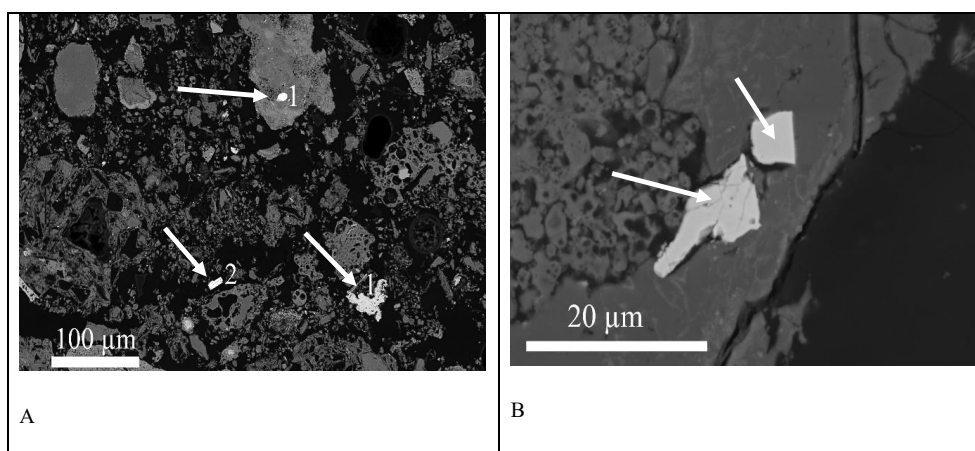


Fig. 6. Sample images from the scanning electron microscopy (SEM) of ash particles from biomass and hard-coal co-combustion: A (WS20) – xenotime (point 1) and zircon (point 2); B (AP20) – monazite

Rys. 6. Przykłady zdjęć ze skaningowego mikroskopu elektronowego (SEM) cząstek popiołów ze współspalania biomasy i węgla kamiennego: A (WS20) – ksenotym (pkt. 1) i cyrkon (pkt. 2); B (AP20) – monacyt

were determined in samples of AP20, AP40 and AP60 ashes, and in their composition La, Nd, and Sm, rarely found next to Ce were Pr and Gd. Almost half of the determined monazite grains contained  $\text{ThO}_2$  in amounts from 4.91% to 12.45%,  $\text{UO}_2$  was rarely determined in them (max. up to 4.73%). In the samples of SH20, SH40 and SH60 ashes, monazite was present in a smaller amount than in the other tested samples of ashes from co-combustion. In all samples of ashes from biomass and hard coal combustion/co-combustion, vitreous aluminosilicate and carbonic substance was determined.

The presence of monazite in ashes from the co-combustion of biomass and hard coal should be associated with the presence of this mineral in hard coal, in which REE are bound by detritic minerals - monazite and xenotime, and appear in the form of admixtures in apatite and zircon (Pindel 2002). In mineral intergrowths of hard coal from USCB, the sources of uranium and thorium are detritic monazite and aggregates of secondary rare earth phosphates with a chemical composition similar to rhabdophane –  $[(\text{Ce},\text{La},\text{Y})\text{PO}_4 \cdot \text{H}_2\text{O}]$  (Pindel 2002). According to Dai et al. (Dai et al. 2014a, 2016) and Zhao et al. (Zhao et al. 2017), the presence of REE in hard coal may be associated with rhabdophane and carbonates containing Ce and Nd. According to Hower et al. (Hower et al. 2020), the presence of REE in hard coal is also associated with florencite  $(\text{CeAl}_3(\text{PO}_4)_2(\text{OH})_6)$ .

Generally, REE in hard coal can be associated with clay minerals, silicates, feldspars, hydroxides, phosphates, carbon and sulphide minerals (Ramakrishna et al. 2018).

According to Franus et al. (Franus et al. 2015) in ashes from Polish power plants, a correlation was found between REE and the content of Al and Si, which indicates vitreous aluminosilicate as a source of REE. Dai et al. (Dai et al. 2014) also associate the presence of La, Ce, Pr, and Nd with some vitreous minerals in ashes. Pyrgaki et al. (Pyrgaki et al. 2021) claim that in hard-coal ashes, a higher concentration of REE was observed in aluminosilicates than in monazite. Pan et al. (Pan et al. 2018) found in ashes from a Chinese power plant that the presence of REY should be associated with silicate and aluminosilicate fractions (65.22%). Hower et al. (Hower et al. 2017), and Smółka-Danielowska (Smółka-Danielowska 2017) determined xenotime containing La, Ce, and Nd in ashes from hard-coal combustion.

Scanning electron microscopy analyses may not be precise for such small ash particles, but they have the advantage of allowing their morphology and chemical composition to be determined on the basis of a large number of determinations.

The tests made it possible to determine the crystalline composition of ashes from biomass combustion, which varies depending on the type of biomass. Based on the phase composition, it was found that ashes from biomass combustion are very diverse and occur in the form of very small particles that are difficult to identify. An important aspect of analyses of biomass ashes is the identification of the aluminosilicate glass phase, which may be the carrier of LREE. In samples from the co-combustion of biomass and hard coal, the source of LREE, apart from monazite, will probably be REE oxides, which may be present in the aluminosilicate glass substance. Further research is needed to confirm this hypothesis.



## Conclusions

The type of biomass and its share in the process of co-combustion with hard coal influence the REY content in ashes; however, the REE content is determined, first of all, by the concentration in hard coal.

The course of the curves of normalized REE concentrations in ashes from the co-combustion of apple pomace (20% and 40% share) and walnut shells (20% and 60% share) with hard coal indicates a certain similarity of these ashes in the distribution of REE.

The ashes from the combustion of apple pomace can be described as type L-M, while the remaining ashes represent type H. The share of critical REE (Nd, Eu, Tb, Dy, Y, and Er) in the samples of ashes from biomass combustion (from 27.7% to 32.1%) is slightly higher than that in hard-coal ash (25.9%). In samples of ashes from biomass and hard-coal co-combustion, the share of critical REE is approx. 31%, regardless of the type of biomass and its share in the combustion process. In these samples of ashes, the values of the prospective coefficient are at a similar level (0.80–0.85), which can be assumed to be a potential material for REE recovery.

Monazite is not the only carrier of REE in ashes from biomass and hard-coal co-combustion, as these elements are probably also present in vitreous aluminosilicate material. The strong correlation between the content of REE and the concentration of  $\Sigma U + Th$ , ambiguously indicates their origin in the ashes.

Ashes from the co-combustion of apple pomace and hard coal should be considered as potentially the most promising in terms of REY content. Further research should be performed in this direction to broaden the knowledge of the presence of REE in various biomass waste materials. It is also necessary to look for new technological processes for REE recovery from ashes in order for this process to become economically viable.

*The Doctoral School partially financed the work at the University of Silesia (Poland) and the funds for statutory research of the Faculty of Natural Sciences.*

## REFERENCES

- Adamczyk et al. 2018 – Adamczyk, Z., Komorek, J., Lewandowska, M., Nowak, J., Białecka, B., Całusz-Moszek, J. and Klupa, A. 2018. Ashes from bituminous coal burning in fluidized bed boilers as a potential source of rare earth elements. *Gospodarka Surowcami Mineralnymi – Mineral Resources Management* 34(2), pp. 21–36. DOI: 10.24425/118652.
- Anshits et al. 2010 – Anshits, N.N. Mikhailova, O.A., Salanov, A.N. and Anshits, A.G. 2010. Chemical composition and structure of the shell of fly ash non-perforated cenospheres produced from the combustion of the Kuznetsk coal (Russia). *Fuel* 89, pp. 1849–1862, DOI: 10.1016/j.fuel.2010.03.049.
- Blissett et al. 2014 – Blissett, R.S., Smalley, N. and Rowson, N.A. 2014. An investigation into six coal fly ashes from the United Kingdom and Poland to evaluate rare earth element content. *Fuel* 119, pp. 236–239, DOI: 10.1016/j.fuel.2013.11.053.

- Bojakowska et al. 2008 – Bojakowska, I., Lech, D. and Wołkowicz, S. 2008. Uranium and thorium in hard and brown coals from Polish deposits (*Uran i tor w węglach kamiennych i brunatnych ze złóż polskich*). *Gospodarka Surowcami Mineralnymi – Mineral Resources Management* 24(2/2), pp. 53–65 (in Polish).
- Całus-Moszek, J. and Białecka, B. 2013. Analysis of the possibilities of rare earth elements obtaining from coal and fly ash (*Analiza możliwości pozyskania pierwiastków ziem rzadkich z węgla kamiennych i popiołów lotnych z elektrowni*). *Gospodarka Surowcami Mineralnymi – Mineral Resources Management* 29(1), pp. 67–80, DOI: 10.2478/gospo-2013-0007 (in Polish).
- Choudhary et al. 2022 – Choudhary, A.K.S., Kumar, S. and Maity, S. 2022. A review on mineralogical speciation, global occurrence and distribution of rare earth and Yttrium (REY) in coal ash. *Journal of Earth System Science* 131, DOI: 10.1007/s12040-022-01913-1.
- Dai et al. 2014 – Dai, S., Zhao, L., Hower, J.C., Johnston, M.N, Song W, Wang P. and Zhang, S. 2014. Petrology, mineralogy, and chemistry of size-fractioned fly ash from the Jungar power plant, Inner Mongolia, China, with emphasis on the distribution of rare earth elements. *Energy Fuels* 28, pp. 1502–1514, DOI: 10.1021/ef402184t.
- Dai et al. 2014a – Dai, S., Luo, Y., Seredin, V.V., Ward, C.R., Hower, J.C., Zhao, L., Liu, S., Tian, H. and Zou, J. 2014a. Revisiting the late Permian coal from the Huayingshan, Sichuan, southwestern China: Enrichment and occurrence modes of minerals and trace elements. *International Journal of Coal Geology* 122, pp. 110–128, DOI: 10.1016/j.coal.2013.12.016.
- Dai et al. 2016 – Dai, S., Liu, J., Ward, C.R., Hower, J.C., French, D., Jia, S., Hood, M.M. and Garrison, T.M. 2016. Mineralogical and geochemical compositions of Late Permian coals and host rocks from the Guxu Coalfield, Sichuan Province, China, with emphasis on enrichment of rare metals. *International Journal of Coal Geology* 166, pp. 71–95, DOI: 10.1016/j.coal.2015.12.004.
- Dai, S. and Finkelman, R.B. 2018. Coal as a promising source of critical elements: Progress and future prospects. *International Journal of Coal Geology* 186, pp.155–164, DOI: 10.1016/j.coal.2017.06.005.
- Eskenazy, G.M. and Stefanova, Y.S. 2007. Trace elements in the Goze Delchev coaldeposit, Bulgaria. *International Journal of Coal Geology* 72(3–4), pp. 257–267, DOI: 10.1016/j.coal.2007.03.002.
- European Commission 2020. A New Industrial Strategy for Europe. Communication from the Commission to the European Parliament, the Council, the European Economic and Social Committee and the Committee of the Regions, COM (2020) 102 Final; European Commission: Brussels, Belgium.
- Franus et al. 2015 – Franus, W., Wiatros-Motyka, M.M. and Wdowin, M. 2015. Coal fly ash as a resource for rare earth elements. *Environmental Science and Pollution Research* 22, pp. 9464–9474, DOI: 10.1007/s11356-015-4111-9.
- Fu et al. 2022 – Fu, B., Hower, J.C., Zhang, W., Luo, G., Hu, H. and Yao, H. 2022. A review of rare elements and yttrium in coal ash: Content, modes of occurrences, combustion behavior, and extraction methods. *Progress in Energy and Combustion Science* 88, DOI: 10.1016/j.pecs.2021.100954.
- GUS – Główny Urząd Statystyczny (Statistic Poland), Ochrona Środowiska 2021. Warszawa (in Polish).
- Hower et al. 2017 – Hower, J.C., Groppo, J.G., Henke, K.R., Graham, U.M., Hood, M.M., Joshi, P. and Preda, D.V. 2017. Ponded and landfilled fly ash as a source of rare earth elements from a Kentucky power plant. *Coal Combustion and Gasification Products* 9, pp. 1–21, DOI: 10.4177/CCGP-D-17-00003.1.
- Hower et al. 2020 – Hower, J.C., Qian, D., Briot, N.J., Hood, M.M. and Eble, C.F. 2020. Nano-scale mineralogy of a Rare earth element-rich Manchester coal lithotype, Clay County, Kentucky. *International Journal of Coal Geology* 220, DOI: 10.1016/j.coal.2019.103413.
- Hower et al. 2021 – Hower, J.C., Groppo, J.G., Jewell, R.F., Wiseman, J.D., Duvallet, T.Y., Oberlink, A.E., Hopps, S.D., Morgan, T.D., Henke, K.R., Joshi, P., Preda, D.V., Gamliel, D.P., Beers, T. and Schrock, M. 2021. Distribution of rare earth elements in the pilot-scale processing of fly ashes derived from eastern Kentucky coals: comparisons of the feed and processed ashes. *Fuel* 295, DOI: 10.1016/j.fuel.2021.120562.
- Jahanban-Esfahlan et al. 2020 – Jahanban-Esfahlan, A., Jahanban-Esfahlan, R., Tabibiazar, M., Roufegarinejad, L. and Amarowicz, R. 2020. Recent advances in the use of walnut (*Juglans regia* L.) shell as a valuable plant-based bio-sorbent for the removal of hazardous materials. *RSC Advances* 10, pp. 7026–7047, DOI: 10.1039/C9RA10084A.
- Jerzak et al. 2021 – Jerzak, W., Murzyn, P., Kuźnia, M. and Magiera, A. 2021. Trace elements retention in bottom ashes during coal combustion with hydrated lime additions. *Energy Sources, Part A: Recovery, Utilization and Environmental Effects* 43(10), pp. 1215–1226, DOI: 10.1080/15567036.2019.1636157.

- Kałużyński et al. 2017 – Kałużyński, M., Jabłoński, S., Kaczmarczyk, J., Świątek, Ł., Pstrowska, K. and Łukasiewicz, M. 2017. Technological aspects of sunflower biomass and brown coal co-firing. *Journal of the Energy Institute*, pp. 1–8, DOI: 10.1016/j.joei.2017.06.003.
- Ketris, M.P. and Yudovich, Y.E. 2009. Estimations of Clarkes for Carbonaceous biolithes: World averages for trace element contents in black shales and coals. *International Journal of Coal Geology* 78, pp. 135–148, DOI: 10.1016/j.coal.2009.01.002.
- Lefcariu et al. 2020 – Lefcariu, L., Klitzing, K.L. and Kolker, A. 2020. Rare Earth Elements and Yttrium (REY) in coal mine drainage from the Illinois Basin, USA. *International Journal of Coal Geology* 217, DOI: 10.1016/j.coal.2019.103327.
- Liu et al. 2019 – Liu, X.M., Hardisty, D.S., Lyons, T.W. and Swart, P.K. 2019. Evaluating the fidelity of the cerium paleoredox tracer during variable carbonate diagenesis on the Great Bahamas Bank. *Geochim Cosmochim Acta* 248, pp. 25–42, DOI: 10.1016/j.gca.2018.12.028.
- Martinez et al. 2018 – Martinez, M., R., Pourret, O., Faucon, M-P., Dian, Ch. 2018. Effect of rare earth elements on rice plant growth. *Chemical Geology* 489, pp. 28–37, DOI: 10.1016/j.chemgeo.2018.05.012.
- Masiarz et al. 2019 – Masiarz, E., Kowalska, H. and Bednarska, M. 2019. The application of plant pomace as a source of dietary fiber and other bio-ingredients in the creation of pro-healthy, sensory and technological properties of baking products® (*Wykorzystanie wytloków roślinnych jako źródła błonnika pokarmowego i innych bio-składników w kreowaniu właściwości prozdrowotnych, sensorycznych i technologicznych pieczywa*). *Postępy Techniki Przetwórstwa Spożywczego* 1, pp. 103–107 (in Polish).
- Mattigod, S.V. 2003. Rare Earth Elements in Fly Ashes as Potential Indicators of Anthropogenic Soil Contamination. [In:] Sajwan, K.S., Alva, A.K., Keefer, R.F. (eds) *Chemistry of Trace Elements in Fly Ash*. Springer, Boston, MA, DOI: 10.1007/978-1-4757-4757-7\_10.
- Miladinović et al. 2020 – Miladinović, M.R., Zdujić, M.V., Veljović, D.N., Kristić, J.B., Banković-Ilić, I.B., Veljković, V.B. and Stamenković, O.S. 2020. Valorization of walnut shell ash as a catalyst for biodiesel production. *Renewable Energy* 147(1), 1033–1043, DOI: 10.1016/j.renene.2019.09.056.
- Ofungwu, J. 2014. Statistical applications for environmental analysis and risk assessment. Wiley and Sons.
- Pan et al. 2018 – Pan, J., Zhou, C., Liu, C., Tang, M., Cao, S., Hu, T., Ji, W., Luo, Y., Wen, M. and Zhang, N. 2018. Modes of occurrence of rare earth elements in coal fly ash – A case study. *Energy Fuels* 32, pp. 9738–9743, DOI: 10.1021/acs.energyfuels.8b0205.
- Pang et al. 2002 – Pang, X., Li, D. and Peng, A. 2002. Application of rare-earth elements in the agriculture of China and its environmental behavior in soil. *Environmental Science and Pollution Research* 9(2), pp. 143–148, DOI: 10.1007/BF02987462.
- Parzenty, H. and Róg, L. 2019. The Role of Mineral Matter in Concentrating Uranium and Thorium in Coal and Combustion Residues from Power Plants in Poland. *Minerals* 9(5), DOI: 10.3390/min9050312.
- Pindel, T. 2002. *Sources of natural radioactivity in selected hard coal mines of the GZW (Źródła promieniotwórczości naturalnej w wybranych kopalniach węgla kamiennego GZW)*. PhD thesis, Katowice: UŚ (in Polish).
- Piyo, N. 2014. *Liquefaction of sunflower husks for biochar production*. Mini-dissertation submitted in partial fulfilment of the requirements for the degree of Masters of Science in Engineering Science in Chemical Engineering in the School of Chemical and Minerals Engineering of the North-West University (Potchefstroom Campus).
- Pyrgaki et al. 2021 – Pyrgaki, K., Gemeni, V., Karkalis, C., Koukoulas, N., Koutsovitis, P. and Petrounias, P. 2021. Geochemical occurrence of rare earth elements in mining waste and mine water: A Review. *Minerals* 11, DOI: 10.3390/min11080860.
- Ramakrishna et al. 2018 – Ramakrishna, C., Thenepalli, T., Nam, Y.S., Kim, Ch. and Ahn, J.W. 2018. The brief review on Coal origin and distribution of rare earth elements in various coal ash sample. *Journal of Energy Engineering* 27(2), pp. 61–69, DOI: 10.5855/ENERGY.2018.27.2.061.
- Rybak, A. and Rybak, A. 2021. Characteristics of some selected methods of rare earth elements recovery from coal fly ashes. *Metals* 11(1), DOI: 10.3390/met110101.
- Schober et al. 2018 – Schober, P., Boer, C. and Schwarte, L.A. 2018. Correlation Coefficients: Appropriate Use and Interpretation. *Anesthesia and Analgesia* 126(5), pp. 1763–1768. DOI: 10.1213/ANE.0000000000002864.
- Seredin, V.V. 2010. A new method for primary evaluation of the outlook for rare earth element ores. *Geology of Ore Deposits* 52, pp. 428–433. DOI: 10.1134/S1075701510050077.

- Seredin, V.V. and Dai, S. 2012. Coal deposits as potential alternative sources for lanthanides and yttrium. *International Journal of Coal Geology* 94, pp. 67–93, DOI: 10.1016/j.coal.2011.11.001.
- Smith et al. 2019 – Smith, R., C., Taggart, R., K., Hower, J., C., Wiesner, M., R. and Hsu-Kim, H. 2019. Selective Recovery of Rare Earth Elements from Coal Fly Ash Leachates Using Liquid Membrane Processes. *Environmental Science and Technology* 53(8), pp. 4490–4499, DOI: 10.1021/acs.est.9b00539.
- Smółka-Danielowska, D. 2013. *Radioactive and rare-earth minerals in fly ashes produced in the process of hard coal combustion (Minerały promieniotwórcze i ziem rzadkich w popiołach wytworzonych w procesie spalania węgla kamiennego)*. Katowice: UŚI. (in Polish).
- Smółka-Danielowska, D. 2017. *The mineralogy and chemistry of fly ashes from Coal Combustion*. [In:] *Environmental science and engineering*. Vol. 7, *Instrumentation, modelling and analysis*. Studium Press LLC, pp. 149–170. ASIN: B083MVCYQH.
- Strzałkowska, E. 2022. Rare earth elements and other critical elements in the magnetic fraction of fly ash from several Polish power plants. *International Journal of Coal Geology* 258, DOI: 10.1016/j.coal.2022.104015.
- Queirós et al. 2020 – Queirós, C.S.G.P., Cardoso, S., Lourenço A., Ferreira J., Miranda I., Lourenço M.J.V. and Pereira H. 2020. Characterization of walnut, almond, and pine nut shells regarding chemical composition and extract composition. *Biomass Conversion and Biorefinery* 10, pp. 175–188, DOI: 10.1007/s13399-019-00424-2.
- Taylor, S.R. and McLennan, S.H. 1985. *The Continental Crust: its Composition and Evolution*. Blackwell Scientific Publications, Oxford.
- Vassilev, S.V. and Vassileva, C.G. 2020. Contents and associations of rare earth elements and yttrium in biomass ashes. *Fuel* 262, DOI: 10.1016/j.fuel.2019.116525.
- Wdowin, M. and Franus, W. 2014. Analysis of fly ash for obtaining rare earth elements (*Analiza popiołów lotnych pod kątem uzyskania z nich pierwiastków ziem rzadkich*). *Polityka Energetyczna – Energy Policy Journal* 17(3), pp. 369–380 (in Polish).
- Zajemska et al. 2017 – Zajemska, M., Urbańczyk, P., Poskart, A., Urbaniak, D., Radomiak, H., Musiał, D., Gołański, G. and Wyleciał, T. 2017. The impact of co-firing sunflower husk pellets with coal in a boiler on the chemical composition of flue gas. *E3S Web of Conferences* 14, DOI: 10.1051/71402021.
- Zhao et al. 2017 – Zhao, L., Dai, S., Graham, I.T., Li, X., Liu, H., Song, X., Hower, J.C. and Zhou, Y. 2017. Cryptic sediment-hosted critical element mineralization from eastern Yunnan Province, southwestern China: Mineralogy, geochemistry, relationship to Emeishan alkaline magmatism and possible origin. *Ore Geology Reviews* 80, pp. 116–140, DOI: 10.1016/j.oregeorev.2016.06.014.
- Zhou et al. 2016 – Zhou, B., Li, Z., Zhao, Y., Zhang, C. and Wei, Y. 2016. Rare Earth Elements supply vs. clean energy technologies: new problems to be solve. *Gospodarka Surowcami Mineralnymi – Mineral Resources Management* 32(4), pp. 29–44, DOI: 10.1515/gospo-2016-0039.
- Żelazny et al. 2020 – Żelazny, S., Świnder, H., Jarosiński, A. and Białecka, B. 2020. The recovery of rare-earth metals from fly ash using alkali pre-treatment with sodium hydroxide. *Gospodarka Surowcami Mineralnymi – Mineral Resources Management* 36(3), pp. 127–144. DOI: 10.24425/gsm.2020.133930.

**RARE EARTH ELEMENTS, URANIUM, AND THORIUM IN ASHES FROM BIOMASS AND HARD-COAL COMBUSTION/CO-COMBUSTION****Keywords**

biomass, hard coal, ash, REY, mineral composition

**Abstract**

This study presents the results of concentrations of rare earth elements and yttrium (REY), uranium (U), and thorium (Th) in ashes from combustion/co-combustion of biomass (20%, 40%, and 60% share) from the agri-food industry (pomace from apples, walnut shells, and sunflower husks) and hard coal. The study primarily focuses on ashes from the co-combustion of biomass and hard coal, in terms of their potential use for the recovery of rare earth elements (REE), and the identification of the sources of these elements in the ashes. Research methods such as ICP-MS (inductively coupled plasma mass spectrometry), XRD (X-ray diffraction), and SEM-EDS (scanning electron microscopy with quantitative X-ray microanalysis) were used. The total average content of REY in ash from biomass combustion is 3.55–120.5 mg/kg, and in ash from co-combustion, it is from 187.3 to 73.5 mg/kg. The concentration of critical REE in biomass combustion ash is in the range 1.0–38.7 mg/kg, and in co-combustion ash it is 23.3–60.7 mg/kg. In hard-coal ash, the average concentration of REY and critical REY was determined at the level of 175 and 45.3 mg/kg, respectively. In all samples of the tested ashes, a higher concentration of Th (0.2–14.8 mg/kg) was found in comparison to U (0.1–6 mg/kg). In ashes from biomass and hard-coal combustion/co-combustion, the range of the prospective coefficient (Coutl) is 0.66–0.82 and 0.8–0.85, respectively, which may suggest a potential source for REE recovery. On the basis of SEM-EDS studies, yttrium was found in particles of ashes from biomass combustion, which is mainly bound to carbonates. The carriers of REY, U, and Th in ashes from biomass and hard-coal co-combustion are phosphates (monazite and xenotime), and probably the vitreous aluminosilicate substance.

**PIERWIĄSTKI ZIEM RZADKICH, URAN I TOR W POPIÓLACH ZE SPALANIA/WSPÓLSPALANIA BIOMASY I WĘGLA KAMIENNEGO****Słowa kluczowe**

biomasa, węgiel kamienny, popiół, REY, skład mineralny

**Streszczenie**

W pracy przedstawiono wyniki stężeń pierwiastków ziem rzadkich i itru (REY), uranu (U), oraz toru (Th) w popiołach ze spalania/współspalania biomasy (udział 20, 40 i 60%) z przemysłu rolno-spożywczego (wytłoki z jabłek, łupiny orzecha włoskiego i łuski słonecznik), i węgla kamiennego. W pracy zwrócono uwagę przede wszystkim na popioły ze współspalania biomasy i węgla kamiennego, pod kątem ich potencjalnego wykorzystania do odzysku pierwiastków ziem rzadkich (REE),

oraz identyfikacji źródeł tych pierwiastków w popiołach. Zastosowano metody badawcze takie jak ICP-MS (spektrometria mas ze wzbudzeniem w plazmie indukcyjnie sprzężonej), XRD (dyfrakcja rentgenowska) i SEM-EDS (skaningowa mikroskopia elektronowa z ilościową mikroanalizą rentgenowską). Całkowita średnia zawartość REY w popiołach ze spalania biomasy wynosi 3,55–120,5 mg/kg, a w popiołach ze współspalania od 73,5 do 187,3 mg/kg. Średnie stężenie krytycznych REE w popiołach ze spalania biomasy mieści się w zakresie 1,0–38,7 mg/kg, a w popiołach ze współspalania 23,3–60,7 mg/kg. W popiele z węgla kamiennego średnie stężenie REY i krytycznych REY oznaczono odpowiednio na poziomie 175 i 45,3 mg/kg. W próbkach badanych popiołów oznaczono wyższe stężenie Th (0,2–14,8 mg/kg), w porównaniu do U (0,1–6 mg/kg). W popiołach ze spalania/współspalania biomasy i węgla kamiennego zakres wartości współczynnika perspektywicznego (Coutl) wynosi odpowiednio 0,66–0,82 i 0,8–0,85, co może sugerować potencjalne źródło do odzysku REE. Analiza cząstek popiołów ze spalania biomasy wykazała itr, który związany jest głównie z węglanami. Nośnikami REY, U i Th w popiołach ze współspalania biomasy i węgla kamiennego są fosforany: monacyt i ksenotym, oraz prawdopodobnie szklista substancja glinokrzemianowa.